HHS Public Access

Author manuscript

*Cell Rep*. Author manuscript; available in PMC 2016 June 02.

Published in final edited form as:

*Cell Rep*. 2016 May 31; 15(9): 2025–2037. doi:10.1016/j.celrep.2016.04.018.

# The lncRNA *SLNCR1* mediates melanoma invasion through a conserved *SRA1*-like region

**Karyn Schmidt**[1,2,3], **Cailin E. Joyce**[1,2,3], **Frank Buquicchio**[1,2,3,*], **Adam Brown**[4], **Justin Ritz**[5], **Robert J. Distel**[6], **Charles H. Yoon**[7,†], and **Carl D. Novina**[1,2,3,†]

[1]Department of Cancer Immunology and Virology, Dana-Farber Cancer Institute, Harvard Medical School, Boston, MA 02115

[2]Department of Microbiology and Immunobiology, Harvard Medical School, Boston, MA 02115

[3]Broad Institute of Harvard and MIT, Cambridge, MA 02141

[4]Department of Biomedical Informatics, Harvard Medical School, Boston, MA 02115

[5]Harvard School of Public Health, Boston, MA 02115

[6]Belfer Office for Dana-Farber Innovation, Dana-Farber Cancer Institute, Boston, MA 02115

[7]Department of Surgery, Brigham and Women's Hospital, Boston, MA 02115, USA

## SUMMARY

Long non-coding RNAs (lncRNAs) have been implicated in numerous physiological processes and diseases, most notably cancers. However, little is known about the mechanism of many functional lncRNAs. We identified an abundantly-expressed lncRNA associated with decreased melanoma patient survival. Increased expression of this lncRNA, *SLNCR1*, mediates melanoma invasion through a highly-conserved sequence similar to the lncRNA *SRA1*. Using a sensitive technique we term RATA (RNA-associated transcription factor array), we show that the brain-specific homeobox protein 3a (Brn3a) and the androgen receptor (AR) bind within and adjacent to *SLNCR1*'s conserved region, respectively. *SLNCR1*, AR, and Brn3a are specifically required for transcriptional activation of matrix metalloproteinase 9 (MMP9) and increased melanoma

[†]corresponding authors: ; Email: chyoon@bics.bwh.harvard.edu, ; Email: carl_novina@dfci.harvard.edu
[*]current address: Northeastern University, Boston, MA 02115

**AUTHOR CONTRIBUTIONS**

K.S., C.E.J., F.B., and C.H.Y. conducted experiments, C.E.J. and A.B. performed bioinformatic analyses, and J.R. was consulted for statistical analyses. Experiments were designed by K.S., R.J.D., and C.D.N. The manuscript was written by K.S. and C.D.N.

**ACCESSION NUMBERS**

The data discussed in this publication have been deposited to the NCBI GEO (Edgar et al., 2002), and the accession number for the data reported in this paper is GEO: GSE77903. Sequencing of patient-derived melanoma and fibroblast STCs can be accessed through the NCBI dbGaP Database of Genotypes and Phenotypes under accession number phs001115.v1.p1.

SUPPLEMENTAL INFORMATION

Supplemental Information includes Extended Experimental Procedures, 7 figures and 6 tables and can be found with this article online.

invasion. Our observations directly link AR to melanoma invasion, possibly explaining why males experience more melanoma metastases and have an overall lower survival as compared to females.

**Keywords**

long non-coding RNA; hormone receptor; melanoma; MMP9; invasion; metastasis

## INTRODUCTION

The incidence of melanoma world-wide has been on the rise for the past 30 years. In the United States, it is estimated that 73,870 new cases will be diagnosed and 9,940 individuals will die of melanoma in 2015 (Siegel et al., 2015). Most early melanomas are easily treated by surgical excision; once metastasized, melanoma is a highly-lethal cancer with a 5-year survival rate of 16% (Howlader N, 2015). Thus, prevention of metastasis is key to melanoma survival and identification of molecular drivers would enable development of novel melanoma therapies.

There is mounting evidence that non-coding RNAs are critical determinants of tumor progression. A major portion (>70,000 genes) of the human non-coding transcriptome is comprised of long non-coding RNAs (lncRNAs) (Zhao et al., 2015). Dysregulated lncRNA expression has recently been linked to many cancers (Li et al., 2013a). LncRNAs may act as oncogenes or tumor suppressors, with an emerging role specifically in cancer metastasis (Serviss et al., 2014). Recent studies implicate lncRNAs in melanomagenesis, though their exact role in melanoma etiology is poorly understood because their molecular and biological functions are obscure (Flockhart et al., 2012; Khaitan et al., 2011; Tang et al., 2013; Tian et al., 2014; Wu et al., 2013).

We profiled lncRNAs expressed in patient-derived melanomas and identified a lncRNA (XLOC_012568) critical for melanoma invasion. This lncRNA contains a conserved ~300 nucleotide region with significant similarity to steroid receptor RNA activator 1 (*SRA1*), and is hence named *SLNCR* (SRA-like non-coding RNA). Survival analysis of The Cancer Genome Atlas (TCGA) melanomas indicates decreased patient survival in patients expressing high levels of *SLNCR*. Knockdown of the most prevalent isoform *SLNCR1* results in the differential expression of 111 transcripts and decreases melanoma invasion. We show that the brain-specific homeobox protein 3a (Brn3a) and the androgen receptor (AR) bind to *SLNCR1*'s conserved sequence and an adjacent sequence, respectively, and that *SLNCR1* coordinates the transcriptional activities of these transcription factors to upregulate the gene encoding the gelatinase MMP9 and increase melanoma invasion. *SLNCR1* binds to and functions with AR, implicating a hormone-responsive transcription factor in melanoma invasion. Thus, our results may reconcile the long-established gender bias in melanoma in which males have a higher frequency of metastases compared to females.

## RESULTS

### *SLNCR* expression is associated with melanoma survival outcome

To identify melanoma-associated lncRNAs, we performed RNA-Sequencing (RNA-seq) on three melanoma short-term cultures (MSTCs) and fibroblast short-term cultures (FSTCs) derived from the tumor microenvironment (unpublished data from Charles Yoon, Brigham and Woman's Hospital, Boston, MA). MSTCs have undergone relatively few passages outside of the patient and closely reflect the genetics of patient melanomas and provide a tractable system to study disease-relevant transcriptional changes. Of the 137 lncRNAs expressed in human melanomas (FPKM > 1, Table S1), the third most abundant lncRNA (XLOC_012568; linc00673, Refseq NR_036488.1; average FPKM = 55.33) is expressed in MSTCs but not FSTCs. Moreover, this lncRNA is located within a chromosomal region commonly amplified in melanoma, lung and ovarian cancers (www.broadinstitute.com/tumorscape, Table S2). We confirmed increased expression of XLOC_012568 in eight MSTCs compared to three normal melanocyte controls by RT-qPCR (Tables S1 and S3, Figure 1A). In addition to melanomas, the MiTranscriptome database (mitranscriptome.org) reveals that XLOC_012568 is increased in lung adenocarcinoma and squamous cell carcinomas compared to corresponding normal tissues, while it is decreased in stomach cancers compared to normal tissues (Iyer et al., 2015) (Figure S1A). XLOC_012568 is also expressed in cervical, ovarian, and pancreatic cancers, low-grade glioma and glioblastoma multiforme. Collectively, these data suggest a broader role for this lncRNA in human tumorigenesis.

There are three XLOC_012568 isoforms expressed in melanomas (Figure S1B). The most prevalent isoform, *SLNCR1*, is 2257 nucleotides and composed of 4 exons spanning chr17:70399463-70588943 (Figure 1B). Isoforms 2 and 3 contain an additional short or long exon, respectively, located between exon 3 and 4. Despite the fact that most lncRNAs display only modest sequence conservation due to their rapid evolution, XLOC_012568 includes a highly-conserved region across mammals (Figures 1B and S1C) (Necsulea et al., 2014). This conserved region is located within a region of high identity (54%) to the steroid receptor RNA Activator-1 (*SRA1*; Figures 1B and S1D). While the *SRA1* locus expresses both protein-coding and functional non-coding transcripts, none of the 3 *SLNCR* isoforms exhibit protein-coding potential (coding potential scores *SLNCR1*: 0.12, *SLNCR2*: 0.10, *SLNCR3*: 0.37) (Chooniedass-Kothari et al., 2004; Kong et al., 2007; Lanz et al., 1999). The conservation of *SLNCR1*, its similarity to another functional non-coding RNA, and its abundant expression across multiple cancers suggests a functionally important role for *SLNCR1*.

To annotate *SLNCR* expression to clinically-relevant parameters, we assessed *SLNCR* expression across 150 randomly-selected human melanomas from TCGA. It is important to note that this analysis does not distinguish between *SLNCR* isoforms. In agreement with results from patient-derived melanomas, *SLNCR* is expressed in 146 out of 150 randomly selected human melanomas (RPKM > 1, Table S1). Tumor depth, as described by Breslow's thickness (T, measured in millimeters), is one of the most important prognostic factors in melanoma treatment. Specifically, while thin tumors (≤1 mm thick) are typically treatable by

surgical excision, thicker tumors (>1 mm thick) have a greater possibility of reaching blood vessels and are thus more likely to metastasize, requiring more aggressive treatment. *SLNCR* expression is significantly higher in tumors at least 1 mm thick, correlating with severity of the melanoma (AJCC staging classification TX/Tis/T0/T1 versus T2/T3/T4; Figure 1C).

To investigate whether *SLNCR* expression is related to disease outcome in TCGA melanomas, we performed a Kaplan-Meier survival analysis comparing melanoma patients expressing high (n = 72, red line) or low (n = 70, blue line) levels of *SLNCR1* defined by the median *SLNCR* expression (Figure 1D). High expression of *SLNCR* is associated with shorter overall survival in melanoma patients (p-value = 0.0426). The median survival for the low *SLNCR* group was 14.3 years, while the high *SLNCR* group had a median survival of only 5.3 years. Additionally, the pooled hazard ratio shows an 84% increase in the risk of death for the high *SLNCR* group (logrank HR = 1.84, 95% confidence interval 1.03 to 3.60). Together, these data suggest a role for *SLNCR* at a clinically-critical stage of melanomagenesis.

### *SLNCR1* increases melanoma invasion by transcriptionally upregulating MMP9

To gain insights into the role of *SLNCR* in melanoma formation, we used global transcriptional profiling before and after knockdown of the most abundant isoform, *SLNCR1,* in the MSTC WM1976. Two custom-designed siRNAs directed against exon 3–4 junction resulted in ~80–90% knockdown of *SLNCR1* (Figures 2A and S2A). Due to toxicity and apparent off-target effects of si-*SLNCR1* (2) 48 hours post-transfection, only differentially expressed transcripts from duplicate knockdown using si-*SLNCR1* (1) were used for RNA-seq analyses (Figure S2B). Knockdown of endogenous *SLNCR1* resulted in the differential expression of 111 transcripts (adjusted p-value < 0.05, fold change >2, Table S4), indicating that *SLNCR1* regulates expression of numerous genes *in trans*.

Next, we assessed whether *SLNCR1* promotes cancer phenotypes in melanoma cells *in vitro*. First, *SLNCR1* expression did not affect viability or proliferation of melanoma cells, as quantified using the metabolic reagent WST-1 (Figures S2B–S2C). Second, *SLNCR1* expression did not significantly alter cell motility, as measured by transwell migration assays (Figure S2D). Finally, we measured invasion using a matrigel invasion assay. *SLNCR1* knockdown significantly decreased invasion in WM1976 (~80%) and WM1575 (~60%) MSTCs, suggesting that endogenous *SLNCR1* plays a critical role in melanoma invasion (Figures 2B and 2C).

To independently validate a role for *SLNCR1* in melanoma invasion, we over-expressed *SLNCR1* in the A375 melanoma cell line. A375 cells express lower levels of *SLNCR1* compared to patient melanomas (Figure 1A), providing a tractable system for mechanistic studies of *SLNCR1* function. As expected, over-expression of *SLNCR1* increased invasion of A375 cells (~200%; Figures 2D and S2E). Over-expression of a *SLNCR1* mutant lacking the highly-conserved sequence (*SLNCR1*$^{\Delta cons}$, nucleotides 462–572 deleted) did not increase invasion, while over-expression of the conserved sequence, including ~100 nucleotides of flanking sequences to ensure proper RNA folding (*SLNCR1*$^{cons}$, nucleotides 372–672), increased invasion to the same degree as full-length *SLNCR1* (~200%; Figure

2D). Collectively, these data indicate that the conserved region is necessary and sufficient for *SLNCR1*-mediated melanoma invasion.

To identify genes that mediate increased melanoma invasion, we over-expressed *SLNCR1*, *SLNCR1*$^{\Delta cons}$, or *SLNCR1*$^{cons}$ in A375 melanoma cells and performed unbiased transcriptional profiling by RNA-seq. Expression of *SLNCR1* resulted in the differential expression of 110 genes (adjusted p-value < 0.05, fold change > 2, Table S5 and Figure S3A). Because the conserved sequence is necessary and sufficient for *SLNCR1*-mediated melanoma invasion, we searched for transcripts differentially expressed upon over-expression of *SLNCR1* and *SLNCR1*$^{cons}$, but not *SLNCR1*$^{\Delta cons}$. Using a less stringent criteria (p-value < 0.05, fold change > 1.5) to ensure identification of all potential candidates, we identified two transcripts significantly upregulated by *SLNCR1*'s conserved sequence: *RARRES2P8*, a pseudogene of the retinoic acid receptor responder, and *MMP9,* a gene that encodes matrix metallopeptidase 9, also known as gelatinase B (Figure 3A). MMP9 contributes to early melanoma invasion through remodeling of the extracellular matrix (Hofmann et al., 2005; MacDougall et al., 1999; MacDougall et al., 1995; van den Oord et al., 1997). Consistent with a role in early tumor dissemination, analysis of our TCGA melanoma cohort revealed that *MMP9* expression is significantly higher in regional metastases compared to primary tumors (p-value = 0.0003, Figure S3B). Furthermore, *SLNCR1* expression in primary melanomas precedes increased *MMP9* expression, supporting *SLNCR1*-regulated expression of *MMP9* (Figure S3B).

Because *SLNCR1*$^{cons}$ regulates expression of MMP9 and mediates *SLNCR1*-induced invasion, we hypothesized that MMP9 is responsible for *SLNCR1*-induced invasion. First, we confirmed that *SLNCR1*$^{cons}$ is necessary and sufficient for increasing MMP9 mRNA (~2.5-fold), as well as MMP9 enzymatic activity (~50%) (Figures 3B and 3C). Over-expression of lncRNAs, like proteins, may force non-physiological interactions and subsequently cause artefactual downstream affects. To confirm that endogenous *SLNCR1* regulates MMP9, we quantified MMP9 expression and activity in MSTCs following *SLNCR1* knockdown. Consistent with a role in regulating MMP9, *SLNCR1* knockdown decreased *MMP9* expression (Log2 fold change = −0.74, Table S4) in WM1976 and decreased MMP9 activity (40–50%) in WM1575 and WM1976 cells (Figures 3D and 3E).

If *SLNCR1* increases melanoma invasion by upregulating MMP9, depleting MMP9 should block *SLNCR1*-mediated invasion. To test this hypothesis, we transfected A375 cells with empty or *SLNCR1*-expressing vectors, along with control or *MMP9*-specific siRNAs (Figure S3C). As expected, *MMP9* knockdown blocked the *SLNCR1*-mediated increase in MMP9 activity and invasion (Figures S3D, S3E, and 3F). These data demonstrate that *SLNCR1* increases melanoma invasion by upregulating MMP9.

LncRNAs can transcriptionally or post-transcriptionally regulate gene expression. To test if *SLNCR1* transcriptionally upregulates *MMP9*, we generated a firefly luciferase (FL) reporter under control of the 2 kilobase *MMP9* promoter (MMP9p-FL) and monitored expression in A375 cells (Figure 3G). When normalized to expression of renilla luciferase from a co-transfected control reporter plasmid, *SLNCR1* expression resulted in a significant (~3.5-fold) increase in FL activity. To further validate the requirement of *SLNCR1*$^{cons}$, we

generated deletion mutants of *SLNCR1* and monitored FL activation. In agreement with previous results showing a requirement of *SLNCR1*$^{cons}$, expression of *SLNCR1*$^{\Delta cons}$ did not increase FL activity. Interestingly, deletion of 70 bases immediately 3′ to the conserved region (*SLNCR1*$^{\Delta 568\text{-}637}$) also failed to increase FL activity, indicating an additional requirement for this sequence in *MMP9* regulation. It is important to note that this region is included in the sequence over-expressed in *SLNCR1*$^{cons}$ (Figure 2D). Furthermore, because serum-containing media contains exogenous hormones and steroids that affect activity of steroid hormone receptors, the assay was performed in the absence of steroids. *SLNCR1* increased FL activity in steroid-deprived cells indicating that *SLNCR1*-mediated regulation of *MMP9* is not dependent on exogenous hormones contained in the media. Collectively, these data confirm that nucleotides 462–637 of *SLNCR1* upregulates the *MMP9* promoter in a ligand-independent manner.

## AR and Brn3a bind to adjacent regions of *SLNCR1*

Previously characterized lncRNAs ‘fine-tune’ gene expression through a range of mechanisms (Geisler and Coller, 2013). We hypothesized that *SLNCR1* binds TFs because *SLNCR1* (1) is expressed in the nucleus (Figure S4A), (2) transcriptionally upregulates the *MMP9* promoter (Figure 3G), and (3) has sequence similarity to *SRA1* (Figure S1D), which has been shown to bind to multiple TFs (Colley and Leedman, 2011). Importantly, TCGA patient melanomas express *SLNCR1* at comparable levels to *SRA1* in other tissues (~0–60 RPKM, or approximately up to 100 copies per cell) (http://gdac.broadinstitute.org) (Harvard, 2015; Kellis et al., 2014; Mortazavi et al., 2008).

Identifying TFs using standard techniques is challenging because of their low expression. We therefore designed a novel method for identifying RNA-bound TFs that we term RATA (RNA-associated transcription factor array). This technique couples an RNA pulldown with a high-throughput TF activation array, enabling highly-sensitive and unbiased identification of TFs bound to an RNA of interest (Figure 4A). The bacteriophage coat protein MS2 interacts with high-affinity to a specific stem-loop structure in the phage genome and has been widely adapted for biochemical purification of mammalian RNAs (Gong and Maquat, 2015). *SLNCR1* constructs containing 12 copies of the MS2 binding sites were co-expressed with a plasmid expressing nuclear FLAG-tagged MS2 protein and immunoprecipitation with anti-FLAG antibodies routinely showed ~30–100 fold enrichment of *SLNCR1* or *SLNCR1*$^{\Delta cons}$ (Figure S4B). For subsequent use in the TF activation array, bound RNAs and proteins were eluted from beads using FLAG peptide under non-denaturing conditions (Figure 4B). The eluate was then subjected to a TF Activation Profiling Plate Array (Signosis), allowing for quantitative analysis of multiple TFs in a single assay. Pulldowns were repeated in triplicate, and TFs showing specific >7-fold enrichment compared to the untagged control in at least 2 experiments were considered potential candidates.

To identify TFs binding to the conserved region of *SLNCR1*, we compared probes enriched from *SLNCR1* versus *SLNCR1*$^{\Delta cons}$ immunoprecipiations. Probes for Brn3a (Pou4F1) routinely showed strong enrichment with *SLNCR1*, but showed negligible enrichment upon deletion of the conserved sequence, suggesting that Brn3a binds to the conserved region. Although Brn3a has not previously been shown to bind RNA, the TF contains a predicted

RNA-binding motif in amino acid position 143–175 (MOTIF Search, http://www.genome.jp/tools/motif/). Importantly, Brn3a has been implicated in melanoma cell cycle progression (Hohenauer et al., 2013).

We also observed modest enrichment of probes specific for the androgen receptor (AR), EGR, E2F-1, ATF2, and AP2. Of these, we focused on AR for several reasons: (1) AP2, ATF2, E2F-1, and EGR directly or indirectly interact with AR (Altintas et al., 2012; Jorgensen and Nilson, 2001; Verger et al., 2001; Zhang et al., 2010), suggesting that enrichment of these probes is a consequence of protein-protein interactions rather than direct interaction with *SLNCR1*. (2) Transcriptional network analysis of melanomas over-expressing or knocking down *SLNCR1* reveals significant enrichment of AR-regulated genes (Table S4: *SLNCR1* knockdown, p-value = 1.45e-59, z-score = 134.17; Table S5: *SLNCR1* over-expression, p-value 5.070E-63, z-score = 160.15; MetaCore™, Thomson Reuters). (3) AR directly binds to other lncRNAs (Yang et al., 2013; Zhang et al., 2015). (4) AR positively regulates MMP9 in other cancers, including gastric, bladder, and prostate cancers (Ergun et al., 2007; Hara et al., 2008; Wang et al., 2013; Wu et al., 2010; Zhang et al., 2014). Notably, (5) melanomas express AR (Allil et al., 2008; Morvillo et al., 2002).

To validate $SLNCR1^{cons}$ binding to AR and Brn3a, we performed RNA immunoprecipitation (RIP) assays in HEK293T (human embryonic kidney) cells, which express very low levels of endogenous *SLNCR1*. *SLNCR1* is significantly enriched (~120-fold) in RNAs immunoprecipitating with ectopically expressed AR (Figure 4D). Surprisingly, $SLNCR1^{\Delta cons}$ is still enriched in AR immunoprecipitates (~50-fold). RNA secondary structure is often critical to RNA function; thus, deletion of the conserved sequence may disrupt adjacent secondary structures and weaken the interaction of AR and *SLNCR1* in the RATA assay. We note that $SLNCR1^{568\text{-}637}$ is required for MMP9 upregulation (Figure 3G), suggesting that AR binds to this region adjacent to the conserved region. Consistent with this hypothesis, $SLNCR1^{\Delta 568\text{-}637}$ is not enriched above background levels of endogenous *SLNCR1* (Figure 4D and data not shown). Taken together, these data confirm that AR binds to $SLNCR1^{568\text{-}637}$.

To capture specific Brn3a-RNA interactions, we used ultraviolet (UV) light to crosslink HEK293T cells prior to immunoprecipitation of Brn3a. *SLNCR1* is significantly enriched in Brn3a immunoprecipitates (~1500-fold) while $SLNCR1^{\Delta cons}$ shows no enrichment (Figure 4E), confirming that Brn3a binds directly to $SLNCR1^{462\text{-}572}$.

## Upregulation of MMP9 requires *SLNCR1*, AR and Brn3a

Because Brn3a binds to *SLNCR1*'s conserved region and AR binds to an adjacent sequence, respectively, we hypothesized that all 3 components are required for upregulation of MMP9 and melanoma invasion. If *SLNCR1* coordinates transcriptional activity of both TFs, MMP9 should not significantly contribute to melanoma invasion in the absence of any single component. It is important to note that in A375 cells, *SLNCR1* is required for MMP9-mediated invasion because knockdown of MMP9 does not decrease invasion of low *SLNCR1*-expressing A375 cells (Figure 3F, vector only samples). To confirm a specific requirement for AR and Brn3a, we repeated gelatin zymography, MMP9p-FL reporter and matrigel invasion assays after over-expressing *SLNCR1* and simultaneously knocking down

of either TF in the A375 melanoma cell line. Consistent with our hypothesis that AR is required for regulating MMP9 activity, depleting AR prevented MMP9 activation and promoter upregulation, as well as melanoma invasion, after *SLNCR1* over-expression (Figures 5A–C and S5A–D). This confirms that AR is required for *SLNCR1*-mediated invasion, even when both Brn3a and *SLNCR1* are present (Figure 5C).

To test if Brn3a is also required for *SLNCR1*-mediated invasion, we repeated the above assays using Brn3a-specific siRNAs. Similar to results seen with AR, depleting Brn3a prevented *SLNCR1*-mediated upregulation of MMP9 activity and promoter upregulation (Figures 5D–E and S5E–G). We also performed invasion assays of A375 melanoma cells expressing vector alone or *SLNCR1* in the presence of scramble or Brn3a-specific siRNAs (Figure 5F). Interestingly, knockdown of Brn3a increased melanoma invasion. However, this increased invasion occurred independently of an increase in *MMP9* (Figures 5D and 5E). Most importantly, expressing *SLNCR1* does not increase melanoma invasion when Brn3a is depleted (Figure 5F, compare bars 3 to 4 and 5 to 6). Thus, our data indicate that Brn3a regulates melanoma invasion through two pathways: one independent of *SLNCR1* and MMP9, and another that requires AR and *SLNCR1* to upregulate MMP9. Because knockdown of AR or Brn3a completely abrogates upregulation of MMP9 and *SLNCR1*-mediated melanoma invasion, our data demonstrates a functional requirement for *SLNCR1*, AR and Brn3a, and suggests formation of a ternary complex composed of *SLNCR1*, AR and Brn3a.

### *SLNCR1* increases AR binding to the *MMP9* promoter

LncRNAs may direct TFs to target regions in the chromosome through direct binding to DNA and formation of an RNA-DNA complex, or by acting as scaffolds to assemble a complex of multiple TFs and regulatory proteins (Geisler and Coller, 2013; Wang and Chang, 2011). We observe no significant similarity between *SLNCR1* and the *MMP9* promoter, arguing against a direct interaction between *SLNCR1* and the DNA. Supporting a model of direct TF binding to *MMP9* promoter elements, the *MMP9* promoter contains multiple functional AREs (androgen response elements), as well as a near perfect consensus Brn3a binding site (gcAT[A/T]A[T/A]T[A/T]AT) (Figure 6A) (Gruber et al., 1997; Zhang et al., 2014). To test if these TF binding sites (TFBSs) are required for *SLNCR1*-mediated transcriptional upregulation of MMP9, we generated MMP9p-FL reporter constructs harboring mutations within the predicted ARE (MMP9p-FL ARE mut) or the Brn3a binding site (MMP9p-FL BBS mut). While over-expression of *SLNCR1* in A375 cells significantly increased luciferase expression from the wild-type MMP9p-FL reporter, mutation of either the predicted Brn3a binding site or the ARE abolished the ability of *SLNCR1* to increase luciferase activity (Figure 6B). These data further suggest formation of a ternary complex composed of *SLNCR1*, AR and Brn3a at the *MMP9* promoter.

Next, we used chromatin immunoprecipitation and PCR (ChIP-PCR) to test if AR directly binds to the *MMP9* promoter. Compared to a vector only control, AR is significantly enriched (~2-fold) at the *MMP9* promoter in the presence of *SLNCR1* (Figure 6C). Collectively, these data indicate that binding of AR, and likely Brn3a, to the *MMP9* promoter is required for transcriptional activation of MMP9.

Finally, we examined our TCGA melanoma cohort for *in vivo* evidence of AR-mediated regulation of *MMP9.* Expression of *AR* and *MMP9* are significantly correlated (r = 0.41, p-value = 0.0003) in high-*SLNCR* melanomas (RPKM ≥ 14.1), but not in low-*SLNCR1* melanomas (RPKM < 14.1), suggesting that AR is bound to the *MMP9* promoter only when *SLNCR1* expression reaches a certain threshold (Figure S6). These data are consistent with AR- and *SLNCR1*-mediated regulation of *MMP9* in patient melanomas.

## DISCUSSION

LncRNAs are emerging as important players in cancer biology; however, the mechanistic details of most lncRNA functions remain unknown. Here, we identify *SLNCR* as a robustly-expressed lncRNA associated with worse overall melanoma survival. *SLNCR1* increases melanoma invasion by transcriptionally upregulating *MMP9*. Our work provides direct biochemical evidence that *SLNCR1* physically interacts with both AR and Brn3a, and that all three components are required for upregulating MMP9. The Brn3a and AR binding sites are located approximately 100 nucleotides apart, an orientation consistent with cooperative TF binding. Our data therefore supports a model in which *SLNCR1* mediates formation of a nuclear *SLNCR1*/AR/Brn3a ternary complex with high affinity for the proximal TFBSs in the *MMP9* promoter (Figure 7). Taken together, this study identifies *SLNCR1* as a novel oncogenic lncRNA with a critical role in melanomagenesis. This finding is in agreement with a recent report in which linc00673 (SLNCR1) was identified as a possible oncogene in non-small-cell lung cancer (Shi et al., 2016).

Although canonical AR activation occurs upon binding of an androgenic hormone ligand, translocation to the nucleus, and AR-dimerization, our data is most consistent with ligand-independent activation of AR and formation of an AR/Brn3a heterodimer. First, *SLNCR1* upregulates the *MMP9* promoter in the absence of exogenous steroids (Figure 3G) or increased nuclear localization of AR (Figure S7A), consistent with ligand-independent activation of AR. Second, if *SLNCR1* induced canonical AR dimerization, over-expression of the lncRNA would increase global activity of AR as opposed only a subset of AR-target genes (Table S5). Third, other AR-associated lncRNAs have been shown to induce AR in a ligand-independent manner (Yang et al., 2013; Zhang et al., 2015). Fourth, AR forms functional heterodimers with other TFs, and was previously shown to directly bind Brn3a in mouse ND7 cells (Berwick et al., 2010; Chen et al., 1997; Lee et al., 1999). These data are consistent with formation of a heterodimer TF complex which significantly increases TF affinity for the tandem TFBSs than either TF alone. An AR monomer has only low affinity for AREs. Similarly, Brn3a has lower affinity for non-consensus TFBSs, such as the one located upstream of MMP9 (Gruber et al., 1997). Formation of an AR/Brn3a heterodimer likely allows for cooperative binding of the TFs to their respective TFBSs, effectively concentrating the nuclear AR in melanoma cells to specific promoters, including the *MMP9* promoter.

It is very difficult to predict lncRNA function based on sequence analysis because lncRNAs are not as conserved as protein-coding genes (Necsulea et al., 2014). However, *SLNCR1* contains a region highly-conserved among mammals that is also similar to a region of *SRA1*, allowing us to extrapolate the function of *SLNCR1*$^{cons}$ from a wide range of

possibilities. In addition to *SRA1*, the lncRNAs *HOTAIR*, and possibly *PRNCR1* and *PCGEM1*, bind to AR (Agoulnik and Weigel, 2009; Prensner et al., 2014; Yang et al., 2013; Zhang et al., 2015). We note a significant sequence similarity between regions of *PCGEM1*, *HOTAIR*, *SLNCR1* and *SRA1* (Figure S7B), suggesting that it is feasible to predict lncRNA function from these sequences. Identification of functional lncRNA sequences may enable determination of the mechanisms of uncharacterized lncRNAs.

While this work has focused on a region of *SLNCR1* with sequence and functional similarities to *SRA1*, there are several important differences between the lncRNAs. (1) *SRA1* has not been implicated in melanoma, and is not differentially expressed between normal melanocytes and melanomas (data not shown). (2) While *SRA1* binds to multiple steroid receptors, including AR, there is no evidence that it interacts with Brn3a or regulates MMP9 (Lanz et al., 1999). (3) Most importantly, siRNA-mediated knockdown of *SLNCR1* does not affect levels of *SRA1* (Figure S2A), indicating that the decrease in invasion (Figures 2B and 2D) and differential gene expression patterns (Table S4) are attributable to depletion of *SLNCR1* and not *SRA1. SLNCR1* therefore functions independently of *SRA1* to regulate melanoma invasion. Identification and analysis of additional functional regions of *SLNCR1* outside of the *SRA1*-like sequence will be an important topic for future studies. For example, *SLNCR1*$^{cons}$ is required for only a small fraction of *SLNCR1*'s gene-regulatory function (Figure S3A). A candidate *SLNCR1*-interacting TF binding outside of its conserved sequence is PAX5, a TF involved in B-cell differentiation (Figure 4C). In addition to TF-dependent functions, *SLNCR1* may have TF-independent functions, such as through interactions with mRNAs, microRNAs or splicing factors, some of which may occur in the cytoplasm (Figure S4A) (Geisler and Coller, 2013).

A gender bias in melanoma biology favoring females was first considered over 40 years ago (Clark et al., 1969). In the years since this study, other studies have confirmed that females have a significant survival advantage compared to males (38%), fewer and delayed metastases, longer delay before relapse, and higher cure rates than males, strongly suggesting a biological basis for the observed gender bias (Bidoli et al., 2012; de Vries et al., 2007; Fisher and Geller, 2013; Gamba et al., 2013; Geller et al., 2002; Joosse et al., 2012; Joosse et al., 2011; Schwartz et al., 2002; Swetter et al., 2009). Differences in expression or activity of sex-hormone receptors, including the estrogen receptor or AR, have long been considered a plausible explanation for the melanoma gender bias (de Giorgi et al., 2011; Morvillo et al., 2002). Recent studies favor a deleterious role for AR and androgens in melanoma, as (1) the female advantage persists even in post-menopausal women, suggesting against an estrogen-related advantage (de Vries et al., 2008; Joosse et al., 2011; Micheli et al., 2009) and (2) there is an increased risk of melanoma following prostate cancer, and vice-versa, suggesting an AR-based connection between the two cancers (Li et al., 2013b; Spanogle et al., 2010). Our results directly implicate AR in melanoma invasion by interacting with *SLNCR1* and upregulating MMP9, possibly reconciling the observation that males suffer an increased number of melanoma metastases.

## EXPERIMENTAL PROCEDURES

### Cell culture

Primary human melanocytes were derived from neonatal foreskins and cultured as previously described (Yokoyama et al., 2008). All other cells were cultured as adherent cells in DMEM (Dulbecco's modified eagle medium, Invitrogen) without glutamine supplemented with 10% fetal bovine serum (FBS). A375 cells were purchased from ATCC, HEK293T cells were a gift from Ronny Drapkin, 'CY' melanomas were a gift from Charles Yoon, and 'WM' melanomas were from collections of the Wistar Institute (Philadelphia, PA). 'CY' melanomas were derived by Charles Yoon.

For luciferase assays, cells were cultured in phenol-red free DMEM without glutamine (Invitrogen), supplemented with 5% charcoal stripped FBS. Luciferase activity was measured using Promega Dual-Glo® Luciferase Assay system. For fractionation experiments, cells were grown to ~80% confluency in 10 cm tissue culture treated dishes and fractionated using Thermo Scientific™ NE-PER™ Nuclear and Cytoplasmic Extraction Kit, according to manufacturer's instructions. Nuclear and cytoplasmic fractions were split for protein and RNA analysis. For proliferation assays, cells were transfected with the indicated siRNAs 24 hours post-seeding and proliferation was measured every 24 hours using WST-1 reagent (Roche) according to the manufacturer's instructions. For chromatin immunoprecipitation and PCR (ChIP-PCR), A375 cells were cultured in phenol-red free DMEM without glutamine (Invitrogen), supplemented with 5% charcoal stripped FBS, and transfected with the indicated plasmid 24 hours post-seeding. Cells were crosslinked in 1% formaldehyde for 15 minutes 48 hours port-transfection, and the reaction was quenched by addition of 0.125 M glycine. ChIP and PCR were performed by Active Motif (Carlsbad, CA). The FKBP5 control primers amplified a region roughly +87015 to the gene, and MMP9 specific primers amplified a region −2254 to the gene.

### Invasion Assays

Cells were plated in either BD BioCoat™ matrigel inserts or uncoated control inserts (Corning) in serum-free media and placed into DMEM with 30% FBS. The number of invaded or migrant cells were imaged on 20x magnification in 8 fields of view for 3 independent replicates.

### Plasmid construction

*SLNCR1* and a codon-optimized Brn3a were synthesized by Biomatik Corporation and cloned into pCDNA3.1 (-). The simian virus nuclear localization signal (SV40-NLS) was cloned upstream of the MS2 ORF in a FLAG-tagged, hMS2-expressing vector, a gift from Dr. Lynne Maquat, University of Rochester Medical Center. Nuclear localization of tagged MS2 was confirmed via fractionation and western blotting. pEGFP-C1-AR was a gift from Michael Mancini (Addgene plasmid # 28235).

### Reagents and antibodies

Lipofectamine® RNAiMax (Life Technologies) was used for all siRNA transfections, and Lipofectamine® 2000 (Life Technologies) was used for all plasmid transfections and

siRNA/plasmid cotransfections. Protein G Dynabeads® (Life Technologies) were used for FLAG-MS2 IPs, and Protein A Dynabeads® (Life Technologies) were used for AR and Brn3a IPs. The following antibodies were used: Sigma Monoclonal ANTI-FLAG® M2 antibody; Santa Cruz AR (N-20), Brn3a (14A6), Hsp90 (4F10), and rabbit IgG control; Cell Signaling GAPDH (14C10); Abcam SNRNP70 (ab83306); and BD Pharmingen™ mouse IgG control. Santa Cruz AR (H-280) was used for ChIP PCR. Sequences for all siRNAs and oligos used in this study can be found in Table S7.

### RNA pulldowns

A375 cells were grown to ~80% confluency in 10 cm dishes, transfected with 10 μg of the plasmid encoding nuclear MS2 and 8 μg of the indicated 3′ MS2 stem-loop tagged *SLNCR1*, and harvested 36–48 hours post-transfection. MS2-tagged *SLNCR1* was confirmed functional by RT-qPCR of selected *SLNCR1* transcriptional targets (data not shown). MS2 RNA pull-downs were completed from non-crosslinked cells a slightly modified protocol from Gong and Maquat ([Gong and Maquat, 2015]). For samples immediately subjected to western blot analysis, beads were resuspended in 25 μl 2X Laemmli sample buffer and incubated at 95°C for 5 minutes. For pulldown extracts subjected to Transcription Factor array analysis, 25 μl of wash buffer containing flag peptide at final concentration of 0.1 mg/ml was added and beads were rotated for 30 minutes at 4°C. Twelve μl of eluate was incubated with biotinylated DNA probe mixture from the Signosis® TF Activation Profiling Plate Array I and subjected to downstream analysis, according to manufacturer's instructions. The signal corresponding to each TF was normalized to that of GATA, and represented as a fold enrichment compared to a cells transfected with a plasmid encoding *SLNCR1* without the MS2 stem loop tag.

RIP assays were performed from HEK293T cells co-transfected with pEGFP-C1-AR or pCDNA-Brn3a and the indicated *SLNCR1* expressing plasmids.

### RNA extraction and cDNA library preparation

RNA was isolated using Trizol® (Life Technologies) and Qiagen RNeasy® Mini Kit and treated with DNase. cDNA was generated using SuperScript III (Invitrogen) reverse transcriptase. The indicated transcripts were quantified using Platinum® SYBR® Green qPCR SuperMix-UDG mix on a CFX384 Touch™ Real-Time PCR Detection System.

The T-test statistics, Pearson correlations, hazard ratio and Kaplan-Meier survival analysis were performed using GraphPad Prism version 6.00 for Windows (GraphPad Software, La Jolla California USA). Image quantifications were performed using ImageJ software.

Please see Extended Experimental Procedures for complete information.

## Supplementary Material

Refer to Web version on PubMed Central for supplementary material.

## Acknowledgments

We gratefully acknowledge T. Benjamin, M. Hemler, M. Brown and the members of our laboratory, especially J. Carroll, for technical advice and critical discussions; D. Fisher for melanocytes; M. Herlyn for melanomas; and R. Rubio, Y. Wang, A. Holman and the entire team of the Dana-Farber Center for Computational Cancer Biology for RNA-Sequencing. This work was supported by funding from NIH R01 CA140986 and R01 CA185151 and a Claudia Adams Barr Award (to C.D.N.) and K.S. was supported by funding from T32 AI007386.

## References

Agoulnik IU, Weigel NL. Coactivator selective regulation of androgen receptor activity. Steroids. 2009; 74:669–674. [PubMed: 19463689]

Allil PA, Visconti MA, Castrucci AM, Isoldi MC. Photoperiod and testosterone modulate growth and melanogenesis of s91 murine melanoma. Med Chem. 2008; 4:100–105. [PubMed: 18336327]

Altintas DM, Shukla MS, Goutte-Gattat D, Angelov D, Rouault JP, Dimitrov S, Samarut J. Direct cooperation between androgen receptor and E2F1 reveals a common regulation mechanism for androgen-responsive genes in prostate cells. Mol Endocrinol. 2012; 26:1531–1541. [PubMed: 22771493]

Berwick DC, Diss JK, Budhram-Mahadeo VS, Latchman DS. A simple technique for the prediction of interacting proteins reveals a direct Brn-3a-androgen receptor interaction. The Journal of biological chemistry. 2010; 285:15286–15295. [PubMed: 20228055]

Bidoli E, Fratino L, Bruzzone S, Pappagallo M, De Paoli P, Tirelli U, Serraino D. Time trends of cancer mortality among elderly in Italy, 1970–2008: an observational study. BMC cancer. 2012; 12:443. [PubMed: 23031713]

Chen S, Wang J, Yu G, Liu W, Pearce D. Androgen and glucocorticoid receptor heterodimer formation. A possible mechanism for mutual inhibition of transcriptional activity. The Journal of biological chemistry. 1997; 272:14087–14092. [PubMed: 9162033]

Chooniedass-Kothari S, Emberley E, Hamedani MK, Troup S, Wang X, Czosnek A, Hube F, Mutawe M, Watson PH, Leygue E. The steroid receptor RNA activator is the first functional RNA encoding a protein. FEBS letters. 2004; 566:43–47. [PubMed: 15147866]

Clark WH Jr, From L, Bernardino EA, Mihm MC. The histogenesis and biologic behavior of primary human malignant melanomas of the skin. Cancer research. 1969; 29:705–727. [PubMed: 5773814]

Colley SM, Leedman PJ. Steroid Receptor RNA Activator - A nuclear receptor coregulator with multiple partners: Insights and challenges. Biochimie. 2011; 93:1966–1972. [PubMed: 21807064]

de Giorgi V, Gori A, Grazzini M, Rossari S, Scarfi F, Corciova S, Verdelli A, Lotti T, Massi D. Estrogens, estrogen receptors and melanoma. Expert Rev Anticancer Ther. 2011; 11:739–747. [PubMed: 21554049]

de Vries E, Houterman S, Janssen-Heijnen ML, Nijsten T, van de Schans SA, Eggermont AM, Coebergh JW. Up-to-date survival estimates and historical trends of cutaneous malignant melanoma in the south-east of The Netherlands. Annals of oncology : official journal of the European Society for Medical Oncology/ESMO. 2007; 18:1110–1116. [PubMed: 17434898]

de Vries E, Nijsten TE, Visser O, Bastiaannet E, van Hattem S, Janssen-Heijnen ML, Coebergh JW. Superior survival of females among 10,538 Dutch melanoma patients is independent of Breslow thickness, histologic type and tumor site. Annals of oncology : official journal of the European Society for Medical Oncology/ESMO. 2008; 19:583–589. [PubMed: 17974555]

Edgar R, Domrachev M, Lash AE. Gene Expression Omnibus: NCBI gene expression and hybridization array data repository. Nucleic acids research. 2002; 30:207–210. [PubMed: 11752295]

Ergun A, Lawrence CA, Kohanski MA, Brennan TA, Collins JJ. A network biology approach to prostate cancer. Molecular systems biology. 2007; 3:82. [PubMed: 17299418]

Fisher DE, Geller AC. Disproportionate burden of melanoma mortality in young U.S. men: the possible role of biology and behavior. JAMA dermatology. 2013; 149:903–904. [PubMed: 23804228]

Flockhart RJ, Webster DE, Qu K, Mascarenhas N, Kovalski J, Kretz M, Khavari PA. BRAFV600E remodels the melanocyte transcriptome and induces BANCR to regulate melanoma cell migration. Genome research. 2012; 22:1006–1014. [PubMed: 22581800]

Gamba CS, Clarke CA, Keegan TH, Tao L, Swetter SM. Melanoma survival disadvantage in young, non-Hispanic white males compared with females. JAMA dermatology. 2013; 149:912–920. [PubMed: 23804160]

Geisler S, Coller J. RNA in unexpected places: long non-coding RNA functions in diverse cellular contexts. Nature reviews Molecular cell biology. 2013; 14:699–712. [PubMed: 24105322]

Geller AC, Miller DR, Annas GD, Demierre MF, Gilchrest BA, Koh HK. Melanoma incidence and mortality among US whites, 1969–1999. Jama. 2002; 288:1719–1720. [PubMed: 12365954]

Gong C, Maquat LE. Affinity Purification of Long Noncoding RNA-Protein Complexes from Formaldehyde Cross-Linked Mammalian Cells. Methods in molecular biology. 2015; 1206:81–86. [PubMed: 25240888]

Gruber CA, Rhee JM, Gleiberman A, Turner EE. POU domain factors of the Brn-3 class recognize functional DNA elements which are distinctive, symmetrical, and highly conserved in evolution. Mol Cell Biol. 1997; 17:2391–2400. [PubMed: 9111308]

Hara T, Miyazaki H, Lee A, Tran CP, Reiter RE. Androgen receptor and invasion in prostate cancer. Cancer research. 2008; 68:1128–1135. [PubMed: 18281488]

Harvard, B.I.o.M.a. Broad Institute TCGA Genome Data Analysis Center: Firehose. 2015.

Hofmann UB, Houben R, Brocker EB, Becker JC. Role of matrix metalloproteinases in melanoma cell invasion. Biochimie. 2005; 87:307–314. [PubMed: 15781317]

Hohenauer T, Berking C, Schmidt A, Haferkamp S, Senft D, Kammerbauer C, Fraschka S, Graf SA, Irmler M, Beckers J, et al. The neural crest transcription factor Brn3a is expressed in melanoma and required for cell cycle progression and survival. EMBO molecular medicine. 2013; 5:919–934. [PubMed: 23666755]

Howlader, N.; NA; Krapcho, M.; Garshell, J.; Miller, D.; Altekruse, SF.; Kosary, CL.; Yu, M.; Ruhl, J.; Tatalovich, Z,Mariotto A.; Lewis, DR.; Chen, HS.; Feuer, EJ.; Cronin, KA. SEER Cancer Statistics Review, 1975–2012. National Cancer Institute; Bethesda, MD: 2015. http://seer.cancer.gov/csr/1975_2012/), pp. based on November 2014 SEER data submission, posted to the SEER web site

Iyer MK, Niknafs YS, Malik R, Singhal U, Sahu A, Hosono Y, Barrette TR, Prensner JR, Evans JR, Zhao S, et al. The landscape of long noncoding RNAs in the human transcriptome. Nature genetics. 2015; 47:199–208. [PubMed: 25599403]

Joosse A, Collette S, Suciu S, Nijsten T, Lejeune F, Kleeberg UR, Coebergh JW, Eggermont AM, de Vries E. Superior outcome of women with stage I/II cutaneous melanoma: pooled analysis of four European Organisation for Research and Treatment of Cancer phase III trials. Journal of clinical oncology : official journal of the American Society of Clinical Oncology. 2012; 30:2240–2247. [PubMed: 22547594]

Joosse A, de Vries E, Eckel R, Nijsten T, Eggermont AM, Holzel D, Coebergh JW, Engel J, Munich Melanoma G. Gender differences in melanoma survival: female patients have a decreased risk of metastasis. The Journal of investigative dermatology. 2011; 131:719–726. [PubMed: 21150923]

Jorgensen JS, Nilson JH. AR suppresses transcription of the alpha glycoprotein hormone subunit gene through protein-protein interactions with cJun and activation transcription factor 2. Mol Endocrinol. 2001; 15:1496–1504. [PubMed: 11518798]

Kellis M, Wold B, Snyder MP, Bernstein BE, Kundaje A, Marinov GK, Ward LD, Birney E, Crawford GE, Dekker J, et al. Defining functional DNA elements in the human genome. Proceedings of the National Academy of Sciences of the United States of America. 2014; 111:6131–6138. [PubMed: 24753594]

Khaitan D, Dinger ME, Mazar J, Crawford J, Smith MA, Mattick JS, Perera RJ. The melanoma-upregulated long noncoding RNA SPRY4-IT1 modulates apoptosis and invasion. Cancer research. 2011; 71:3852–3862. [PubMed: 21558391]

Kong L, Zhang Y, Ye ZQ, Liu XQ, Zhao SQ, Wei L, Gao G. CPC: assess the protein-coding potential of transcripts using sequence features and support vector machine. Nucleic acids research. 2007; 35:W345–349. [PubMed: 17631615]

Lanz RB, McKenna NJ, Onate SA, Albrecht U, Wong J, Tsai SY, Tsai MJ, O'Malley BW. A steroid receptor coactivator, SRA, functions as an RNA and is present in an SRC-1 complex. Cell. 1999; 97:17–27. [PubMed: 10199399]

Lee YF, Shyr CR, Thin TH, Lin WJ, Chang C. Convergence of two repressors through heterodimer formation of androgen receptor and testicular orphan receptor-4: a unique signaling pathway in the steroid receptor superfamily. Proceedings of the National Academy of Sciences of the United States of America. 1999; 96:14724–14729. [PubMed: 10611280]

Li J, Xuan Z, Liu C. Long non-coding RNAs and complex human diseases. International journal of molecular sciences. 2013a; 14:18790–18808. [PubMed: 24036441]

Li WQ, Qureshi AA, Ma J, Goldstein AM, Giovannucci EL, Stampfer MJ, Han J. Personal history of prostate cancer and increased risk of incident melanoma in the United States. Journal of clinical oncology : official journal of the American Society of Clinical Oncology. 2013b; 31:4394–4399. [PubMed: 24190118]

MacDougall JR, Bani MR, Lin Y, Muschel RJ, Kerbel RS. 'Proteolytic switching': opposite patterns of regulation of gelatinase B and its inhibitor TIMP-1 during human melanoma progression and consequences of gelatinase B overexpression. British journal of cancer. 1999; 80:504–512. [PubMed: 10408860]

MacDougall JR, Bani MR, Lin Y, Rak J, Kerbel RS. The 92-kDa gelatinase B is expressed by advanced stage melanoma cells: suppression by somatic cell hybridization with early stage melanoma cells. Cancer research. 1995; 55:4174–4181. [PubMed: 7664294]

Micheli A, Ciampichini R, Oberaigner W, Ciccolallo L, de Vries E, Izarzugaza I, Zambon P, Gatta G, De Angelis R, Group EW. The advantage of women in cancer survival: an analysis of EUROCARE-4 data. European journal of cancer. 2009; 45:1017–1027. [PubMed: 19109009]

Mortazavi A, Williams BA, McCue K, Schaeffer L, Wold B. Mapping and quantifying mammalian transcriptomes by RNA-Seq. Nature methods. 2008; 5:621–628. [PubMed: 18516045]

Morvillo V, Luthy IA, Bravo AI, Capurro MI, Portela P, Calandra RS, Mordoh J. Androgen receptors in human melanoma cell lines IIB-MEL-LES and IIB-MEL-IAN and in human melanoma metastases. Melanoma research. 2002; 12:529–538. [PubMed: 12459642]

Necsulea A, Soumillon M, Warnefors M, Liechti A, Daish T, Zeller U, Baker JC, Grutzner F, Kaessmann H. The evolution of lncRNA repertoires and expression patterns in tetrapods. Nature. 2014; 505:635–640. [PubMed: 24463510]

Prensner JR, Sahu A, Iyer MK, Malik R, Chandler B, Asangani IA, Poliakov A, Vergara IA, Alshalalfa M, Jenkins RB, et al. The lncRNAs PCGEM1 and PRNCR1 are not implicated in castration resistant prostate cancer. Oncotarget. 2014; 5:1434–1438. [PubMed: 24727738]

Schwartz JL, Wang TS, Hamilton TA, Lowe L, Sondak VK, Johnson TM. Thin primary cutaneous melanomas: associated detection patterns, lesion characteristics, and patient characteristics. Cancer. 2002; 95:1562–1568. [PubMed: 12237926]

Serviss JT, Johnsson P, Grander D. An emerging role for long non-coding RNAs in cancer metastasis. Frontiers in genetics. 2014; 5:234. [PubMed: 25101115]

Shi X, Ma C, Zhu Q, Yuan D, Sun M, Gu X, Wu G, Lv T, Song Y. Upregulation of long intergenic noncoding RNA 00673 promotes tumor proliferation via LSD1 interaction and repression of NCALD in non-small-cell lung cancer. Oncotarget. 2016; 7(18):25558–25575.

Siegel RL, Miller KD, Jemal A. Cancer statistics, 2015. CA: a cancer journal for clinicians. 2015; 65:5–29. [PubMed: 25559415]

Spanogle JP, Clarke CA, Aroner S, Swetter SM. Risk of second primary malignancies following cutaneous melanoma diagnosis: a population-based study. Journal of the American Academy of Dermatology. 2010; 62:757–767. [PubMed: 20223559]

Swetter SM, Layton CJ, Johnson TM, Brooks KR, Miller DR, Geller AC. Gender differences in melanoma awareness and detection practices between middle-aged and older men with melanoma and their female spouses. Archives of dermatology. 2009; 145:488–490. [PubMed: 19380679]

Tang L, Zhang W, Su B, Yu B. Long noncoding RNA HOTAIR is associated with motility, invasion, and metastatic potential of metastatic melanoma. BioMed research international. 2013; 2013:251098. [PubMed: 23862139]

Tian Y, Zhang X, Hao Y, Fang Z, He Y. Potential roles of abnormally expressed long noncoding RNA UCA1 and Malat-1 in metastasis of melanoma. Melanoma research. 2014

van den Oord JJ, Paemen L, Opdenakker G, de Wolf-Peeters C. Expression of gelatinase B and the extracellular matrix metalloproteinase inducer EMMPRIN in benign and malignant pigment cell lesions of the skin. The American journal of pathology. 1997; 151:665–670. [PubMed: 9284814]

Verger A, Buisine E, Carrere S, Wintjens R, Flourens A, Coll J, Stehelin D, Duterque-Coquillaud M. Identification of amino acid residues in the ETS transcription factor Erg that mediate Erg-Jun/Fos-DNA ternary complex formation. The Journal of biological chemistry. 2001; 276:17181–17189. [PubMed: 11278640]

Wang KC, Chang HY. Molecular mechanisms of long noncoding RNAs. Molecular cell. 2011; 43:904–914. [PubMed: 21925379]

Wang X, Lee SO, Xia S, Jiang Q, Luo J, Li L, Yeh S, Chang C. Endothelial cells enhance prostate cancer metastasis via IL-6-->androgen receptor-->TGF-beta-->MMP-9 signals. Mol Cancer Ther. 2013; 12:1026–1037. [PubMed: 23536722]

Wu CF, Tan GH, Ma CC, Li L. The non-coding RNA llme23 drives the malignant property of human melanoma cells. Journal of genetics and genomics = Yi chuan xue bao. 2013; 40:179–188. [PubMed: 23618401]

Wu JT, Han BM, Yu SQ, Wang HP, Xia SJ. Androgen receptor is a potential therapeutic target for bladder cancer. Urology. 2010; 75:820–827. [PubMed: 20083299]

Yang L, Lin C, Jin C, Yang JC, Tanasa B, Li W, Merkurjev D, Ohgi KA, Meng D, Zhang J, et al. lncRNA-dependent mechanisms of androgen-receptor-regulated gene activation programs. Nature. 2013; 500:598–602. [PubMed: 23945587]

Yokoyama S, Feige E, Poling LL, Levy C, Widlund HR, Khaled M, Kung AL, Fisher DE. Pharmacologic suppression of MITF expression via HDAC inhibitors in the melanocyte lineage. Pigment Cell Melanoma Res. 2008; 21:457–463. [PubMed: 18627530]

Zhang A, Zhao JC, Kim J, Fong KW, Yang YA, Chakravarti D, Mo YY, Yu J. LncRNA HOTAIR Enhances the Androgen-Receptor-Mediated Transcriptional Program and Drives Castration-Resistant Prostate Cancer. Cell Rep. 2015; 13:209–221. [PubMed: 26411689]

Zhang BG, Du T, Zang MD, Chang Q, Fan ZY, Li JF, Yu BQ, Su LP, Li C, Yan C, et al. Androgen receptor promotes gastric cancer cell migration and invasion via AKT-phosphorylation dependent upregulation of matrix metalloproteinase 9. Oncotarget. 2014; 5:10584–10595. [PubMed: 25301736]

Zhang J, Gonit M, Salazar MD, Shatnawi A, Shemshedini L, Trumbly R, Ratnam M. C/EBPalpha redirects androgen receptor signaling through a unique bimodal interaction. Oncogene. 2010; 29:723–738. [PubMed: 19901962]

Zhao Y, Li H, Fang S, Kang Y, Wu W, Hao Y, Li Z, Bu D, Sun N, Zhang MQ, et al. NONCODE 2016: an informative and valuable data source of long non-coding RNAs. Nucleic acids research. 2015

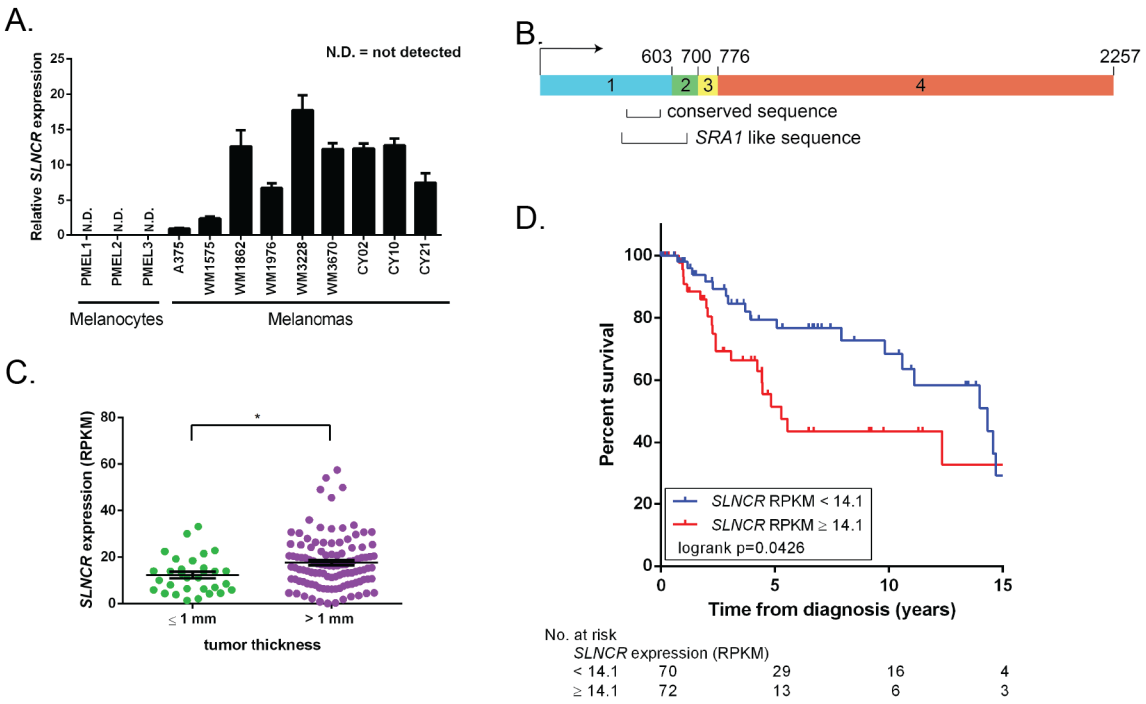


**Figure 1. *SLNCR* is expressed in melanomas and is associated with worse overall survival**

(A) Relative expression of *SLNCR* across multiple melanocytes and melanomas, as measured by RT-qPCR, compared to A375 after normalization to *GAPDH*. Error bars represent standard deviations calculated from 3 reactions. (B) Schematic presentation of *SLNCR1*'s exon structure. The highly-conserved and *SRA1*-like sequences are highlighted. (C) Box plot of *SLNCR* expression from 150 TCGA melanomas categorized based on tumor thickness at diagnosis. Data are represented as mean ± SEM. Significance was calculated using the Student's t-test: * p-value < 0.05. (D) Kaplan-Meier survival analysis of high or low *SLNCR* expressing TCGA melanomas, defined by the median *SLNCR* expression (RPKM = 14.1). See also Figure S1.

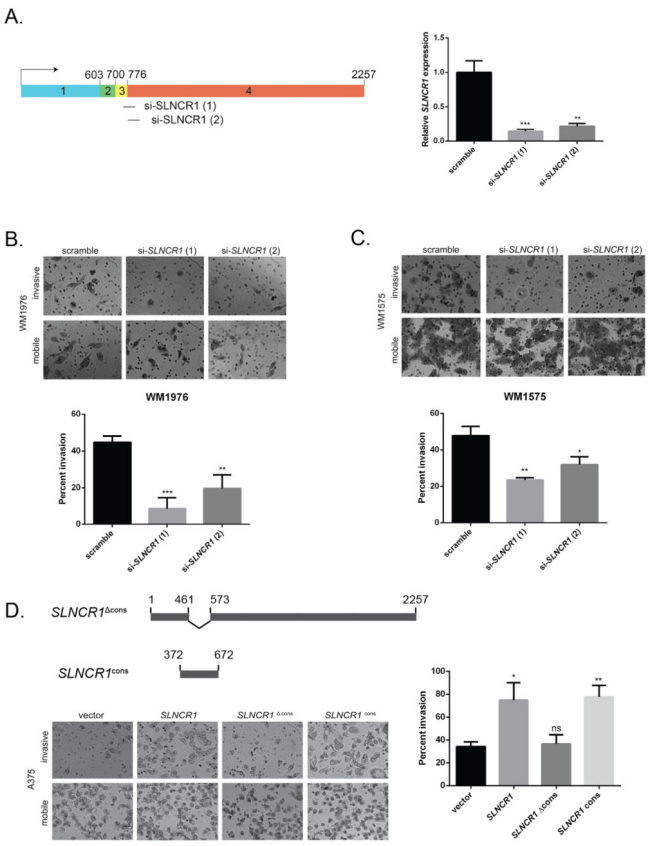


**Figure 2. *SLNCR*'s highly-conserved sequence increases melanoma invasion**

(A) Schematic presentation of *SLNCR1*-specific siRNAs targeting the exon 3–4 junction. Right: relative expression of *SLNCR1* upon siRNA knockdown in the MSTC WM1976. RT-qPCR data is represented as the fold change compared to scramble siRNA control, normalized to *GAPDH*. Error bars represent standard deviations calculated from 3 reactions. (B–C) Matrigel invasion assays of WM1976 (B) or WM1575 (C) cells transfected with the indicated siRNA. Invasion is calculated as the percent of invading cells compared to mobile cells as counted in 8 fields of view. Top panels show representative images of the indicated invading and mobile cells. Quantification from 3 independent replicates, represented as mean ± SD, is shown at the bottom. (D) As in (B and C) but with A375 melanoma cells transfected with the indicated plasmids. The schematic presentation (top) denotes the *SLNCR1* sequences expressed from the indicated plasmids. The bottom left panel shows representative images, while quantification from 3 independent replicates is shown at the right. Significance was calculated using the Student's t-test: * p-value < 0.05, ** p-value < 0.005, *** p-value < 0.0005, ns = not significant. See also Figure S2.

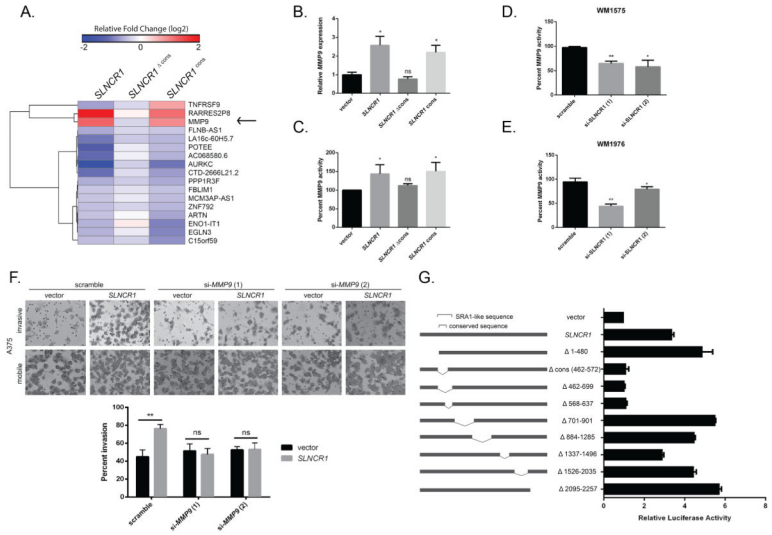


**Figure 3. *SLNCR1* increases melanoma invasion by transcriptionally upregulating MMP9**

(A) Heat map of differentially expressed genes significantly regulated by *SLNCR1* and *SLNCR1*$^{cons}$, but not *SLNCR1*$^{\Delta cons}$, in the melanoma cell line A375. The shading represents the log2 fold change compared vector only control. (B) Relative *MMP9* expression in A375 cells transfected with the indicated plasmids. RT-qPCR data is represented as the fold change compared to a vector control, normalized to *GAPDH*. Error bars represent standard deviations calculated from 3 reactions. (C–E) MMP9 activity from supernatants of cells transfected with the indicated plasmids or siRNAs were quantified using gelatin zymography. Percent MMP9 activity is represented as fold change compared to the vector or scramble control, normalized to MMP2 activity. Error bars represent standard deviations from three independent replicates. (C) Percent MMP9 activity in supernatants of A375 cells transfected with the indicated plasmids. (D) Percent MMP9 activity of WM1976 supernatant upon knockdown of *SLNCR1*. (E) Percent MMP9 activity of WM1575 supernatant upon knockdown of *SLNCR1*. (F) Matrigel invasion assay of A375 melanoma cells transfected with the indicated plasmids and siRNAs, as in Figure 2 (B–D). (G) A375 cells, grown in steroid-deprived conditions, were transfected with a MMP9p-firefly (FL) reporter plasmid, a CMV-RL (renilla luciferase) control, and the indicated *SLNCR1* expression plasmids. Luciferase activity was measured 24 hours post-transfection. Relative FL activity was calculated as a fold-change compared to vector only control cells, after normalization to RL activity. Shown is one representative assay from at least three independent replicates. Error bars represent standard deviation from four reactions. Significance was calculated using the Student's t-test: * p-value < 0.05, ** p-value < 0.005, *** p-value < 0.0005, ns = not significant. See also Figure S3.

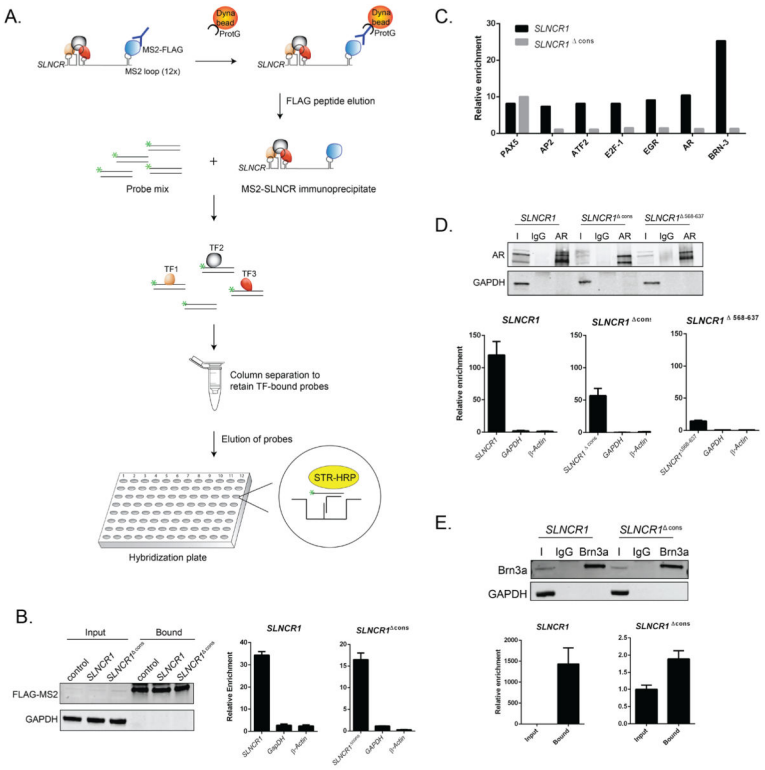


**Figure 4. AR and Brn3a bind to adjacent *SLNCR1* sequences**

(A) Schematic presentation of the RATA method for identifying TFs associated with *SLNCR1. SLNCR1*-MS2 RNP complexes were immunoprecipitated with α-FLAG antibody, eluted from beads using FLAG peptide, and the eluate was immediately subjected to the TF Activation Profiling Plate Array I (Signosis). TF-bound probes were isolated through column separation and analyzed through hybridization with a plate whose wells are pre-coated with complementary DNA. (B) Ectopically expressed FLAG-tagged MS2 was immunoprecipitated from A375 cells transfected with the indicated MS2-loop containing *SLNCR1* construct, compared to control cells expressing untagged *SLNCR1* constructs. Left panel: total protein input or bound proteins following IP with α-FLAG antibody was subjected to Western blot analysis. The blot was probed with α-FLAG and α-GAPDH antibodies. Middle and right: relative enrichment of the indicated transcripts as measured by RT-qPCR compared to RNA enriched from cells expressing *SLNCR1* without MS2 stem loops. Bound FLAG-MS2 RNPs were eluted using FLAG peptide. (C) Fold enrichment of TF-specific probes with MS2-based purification of *SLNCR1* or *SLNCR1*$^{\Delta cons}$ from A375 cells. Probe enrichment is represents fold enrichment compared to an untagged RNA control IP, after normalization to the signal of GATA-specific probes. Shown is one representative assay of TF-specific probes showing significant (>7-fold) enrichment in at least two out of three replicates. (D) Immunoprecipitations from HEK293T transfected with GFP-tagged AR and the indicated *SLNCR1* expressing plasmids using either α-AR antibody or an IgG nonspecific control. Top panel: western blot analysis of input (I), IgG bound (IgG) or α-AR bound (AR) proteins. Bottom panels: relative enrichment of the indicated transcripts from AR-IPs, compared to an IgG nonspecific control. HEK293T cells were transfected with GFP-tagged AR and either *SLNCR1* (bottom left panel) or *SLNCR1* $^{\Delta cons}$ (bottom middle

panel) or *SLNCR1* $^{\Delta 568\text{-}637}$(bottom right panel) expression plasmids. (E) Immunoprecipitations from UV-crosslinked HEK293T transfected with Brn3a and the indicated *SLNCR1* expression plasmid using either anti-Brn3a antibody or an IgG nonspecific control. Top panel: western blot of input (I), IgG bound (IgG) or α-Brn3a bound (Brn3a) proteins. Bottom panels: relative enrichment of the indicated transcripts from Brn3a-IPs. HEK293T cells were transfected with Brn3a and either *SLNCR1* (bottom left panel) or *SLNCR1* $^{\Delta cons}$ (bottom right panel). To control for differences in the efficiency of proteinase K digestion, enrichment was calculated compared to input transcript levels after normalization to levels of the 18s RNA. All RT-qPCR are represented as mean ± SD from three replicates. See also Figure S4.

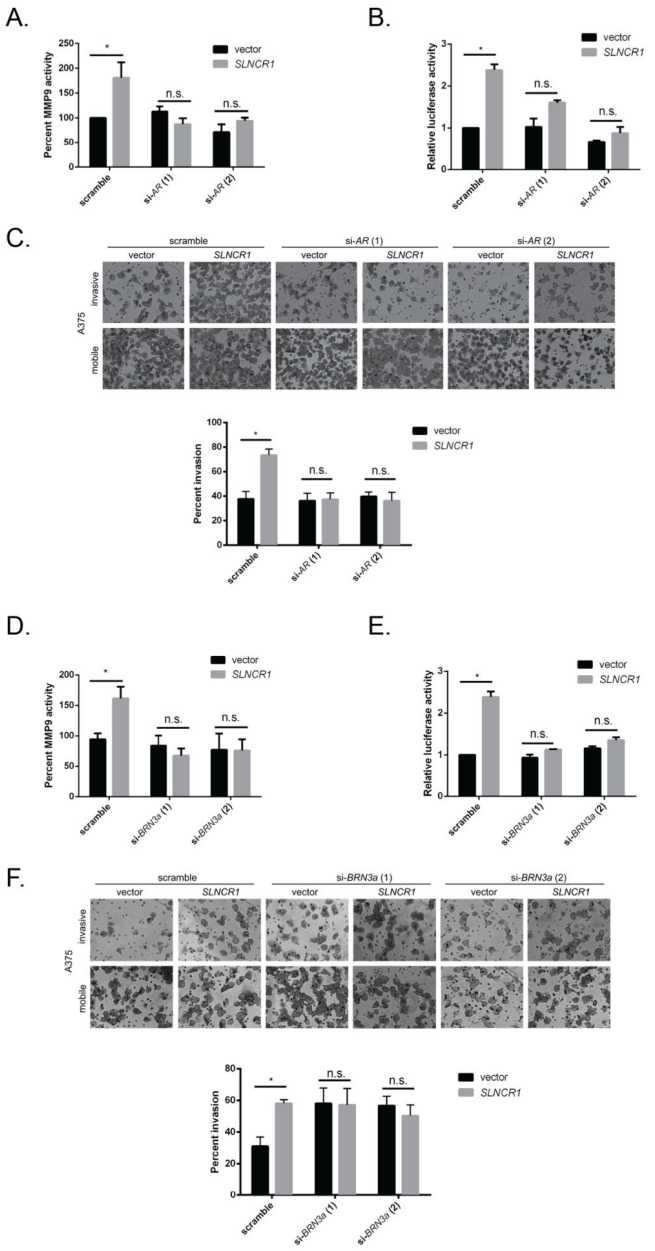


**Figure 5. *SLNCR1* mediated invasion requires AR and Brn3a**

(A and D) MMP9 activity of A375 cells transfected with the indicated plasmids and siRNAs, as in Figure 3 (C–E). (B and E) Relative luciferase activity of A375 cells transfected with an MMP9-RL reporter, as well as the indicated plasmids and siRNAs. Quantification was performed as in Figure 3G. (C and F) Matrigel invasion assay of A375 melanoma cells transfected with the indicated plasmids and siRNAs. The top panel shows representative images of the indicated invading or mobile cells, and the quantification from 3 independent replicates is shown at the bottom. Significance was calculated using the Student's t-test: * p-value < 0.05, n.s. = not significant. See also Figure S5.

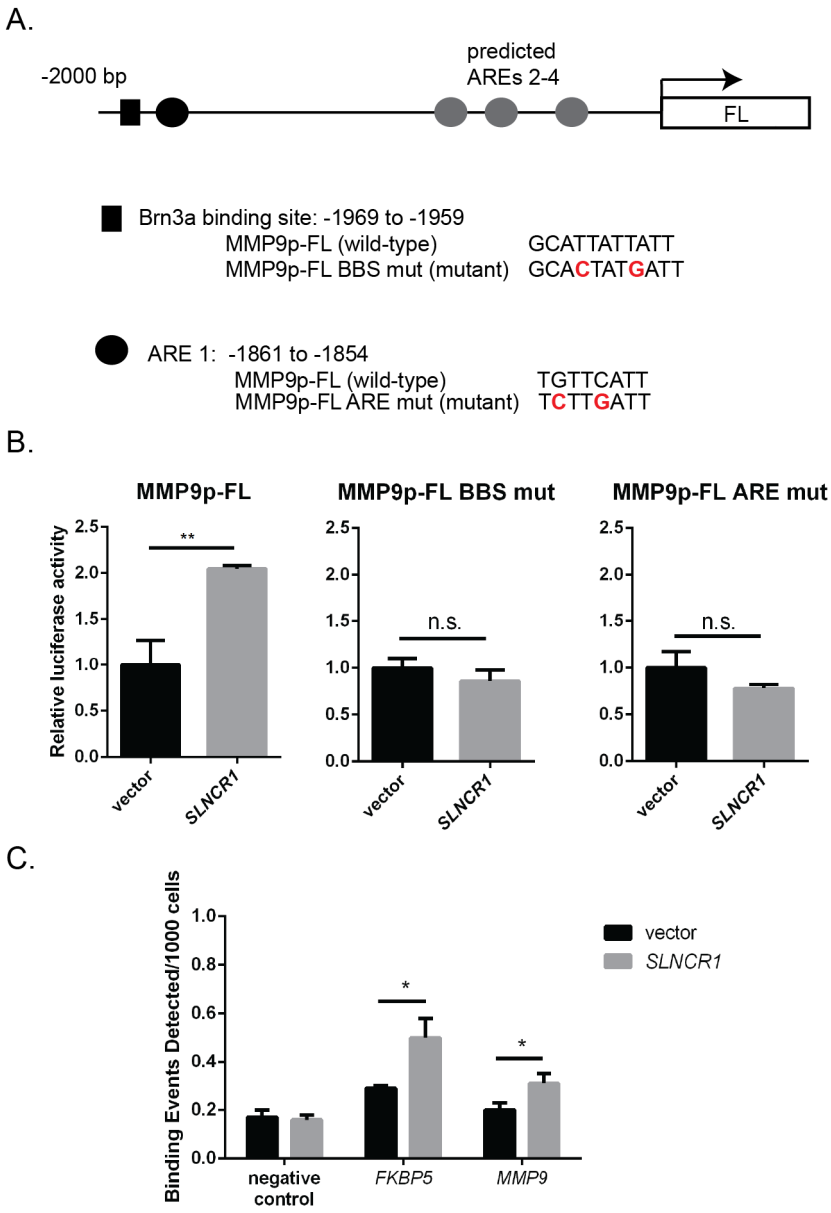


**Figure 6. AR and Brn3a binding sites are required for *SLNCR1*-induced upregulation of the *MMP9* promoter**

(A) Schematic presentation of the 2 KB MMP9 promoter cloned upstream of the firefly luciferase reporter. The black box denotes a predicted Brn3a binding site. The wild-type and mutated sequences are shown below. The black circle denotes a functional ARE, with wild-type and mutated sequences below. The grey circles denote additional predicted AREs. (B) Mutation of either the Brn3a binding site (MMP9p-FL BBS mut) or the ARE (MMP9p-FL ARE mut) prevents *SLNCR1*-mediated upregulation of the MMP9 promoter. Assay was completed as in Figure 3G. Error bars represent standard deviation from four reactions. (C) AR-ChIP from A375 cells transfected with either vector or *SLNCR1*-expressing plasmid. qPCR was performed using primers specific to the regions indicated, including primers

corresponding to a gene desert (negative control). * p-value < 0.05, ** p-value < 0.005, n.s. = not significant. See also Figure S6.

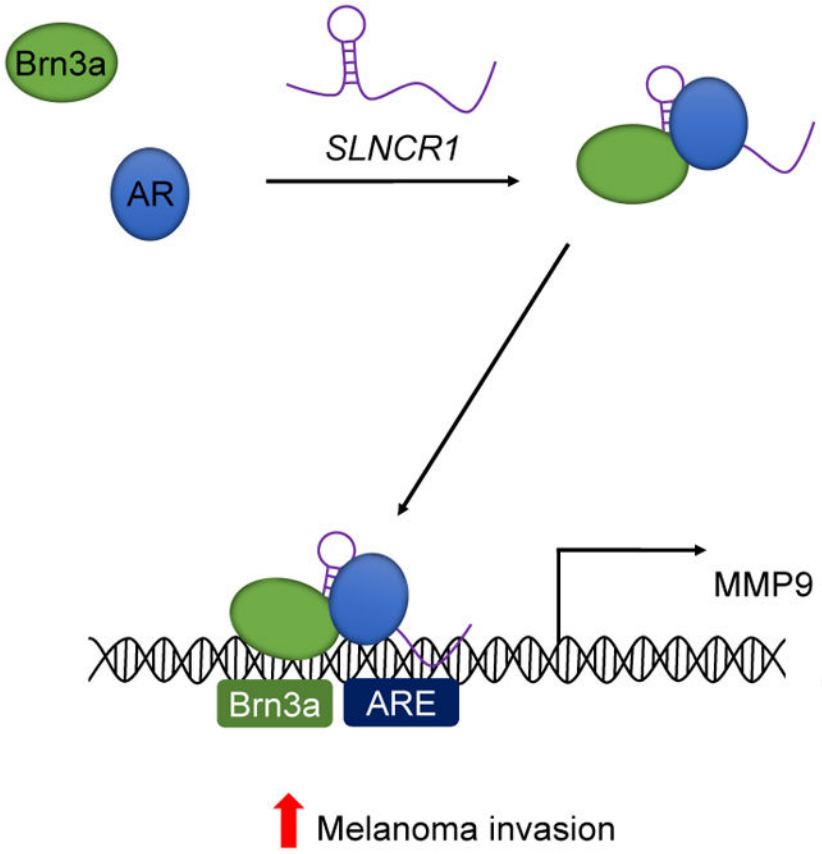


**Figure 7. Model for *SLNCR1*-induced MMP9 transcriptional upregulation**

When *SLNCR1* increases, AR and Brn3a bind to conserved, adjacent regions of *SLNCR1.* The *SLNCR1*/AR/Brn3a ternary complex has high affinity for adjacent Brn3a and AR binding sites located upstream of the *MMP9* transcriptional start site. Cooperative binding of AR and Brn3a to its promoter increases MMP9 expression and activity and thus increases invasion of melanoma cells. See also Figures S7.